

Adsorptive Removal of Salicylic Acid from Aqueous Solutions using New Graphene-Based Nanosorbents

Xin Jiat Lee, Nishanth Chemmangattuvalappil, Lai Yee Lee*

Department of Chemical and Environmental Engineering, Faculty of Engineering, University of Nottingham Malaysia Campus, Jalan Broga, 43500 Semenyih, Selangor, Malaysia
laiyee-lee@nottingham.edu.my

In the present research, new carbon nanosorbents were developed for removal of salicylic acid (SA) in aqueous media. The starting materials were graphene flakes with thicknesses of 12 nm (C12) and 60 nm (C60) subjected to covalent functionalisation in a reflux reactor using different chemical reagents (HNO₃, H₂SO₄, NaOH and KOH) at 353 K for 4 h. Characterisation work revealed that the specific surface areas of C12 and C60 were 68.74 and 9.76 m²/g, respectively. The capability of the prepared nanosorbents in SA sequestration was examined using batch adsorption system. The results suggested that C12 treated with H₂SO₄ (C12-H₂SO₄) exhibited the highest percentage removal of SA (55 %). FTIR analysis showed the presence of various functional groups *viz.* hydroxyl, alkyne, amine, carboxylic acid, carbonyl, alcohol and alkyl halide on C12-H₂SO₄ which might have interacted with SA. The adsorption equilibrium was evaluated by varying the initial SA concentration. Experimental data were analysed by Langmuir, Temkin and Dubinin-Radushkevich (D-R) and Freundlich models. The goodness-of-fit of the models was determined by Marquardt's percent standard deviation, chi-square, average relative error and sum of absolute error with model parameter optimisation evaluated by sum of normalised errors (SNE). It was found that D-R model was the best fit model with the lowest SNE. The primary results showed that chemical functionalisation has been successfully used for attaching specific functional groups onto C12. In addition, the new graphene-based nanosorbent *viz.* C12-H₂SO₄ has a great potential application for SA removal.

1. Introduction

Pollution of aquatic ecosystems caused by pharmaceutical residues is an emerging environmental issue due to their harmful effects on human health and other organisms. Among the pharmaceutical pollutants, salicylic acid (SA) is most frequently detected in hospital waste and pharmaceutical industry effluents. SA is an anti-inflammatory drug commonly used to treat acne, wart and fungus infections (Jiang et al., 2013). However, when exposed to high doses, SA can cause severe health problems such as salicylate poisoning, nausea, delirium, coma, severe stomach ache, gastric and death (Otero et al., 2004). The presence of SA in water resources is thus a serious concern, and its removal from industrial effluent is crucial to safeguard human health and the environment.

Numerous techniques have been used for treating water media contaminated with conventional pollutants and these include membrane filtration, advanced oxidation, electrochemical and biological processes. These methods however, suffer from disadvantages such as formation of recalcitrant by-products, expensive and ineffectiveness in treating effluent with low concentration of pollutants. Adsorption is a promising abatement technique for this emerging class of pollutant as it is relatively easy to operate, efficient and does not form any by-products (Alvarez et al., 2013). In addition, both the treated water and the regenerated adsorbent can be reused. Various adsorbents have been tested on the removal of pharmaceutical pollutants such as polymeric resins (Turku et al., 2009), biochar (Essandoh et al., 2015), activated carbon (Otero et al., 2004) and zeolites (Martucci et al., 2012). However, there is an on-going search for more efficient and robust adsorbents for the removal of this pollutant class.

Graphene is a new fascinating carbon nanomaterial which has garnered a great deal of interest as nanosorbent precursor for pollution control applications in recent years. It is a 2-dimensional layer of sp²

hybridised carbon atoms. Graphene offers significant improvement in nanosorbent design owing to its exceptionally high specific surface area, numerous sorption sites, low temperature modification, short intraparticle diffusion path length, better regeneration and reusability properties than commercial adsorbents. Furthermore, graphene has relatively large and delocalised π -electron system which may possess binding attributes for target pollutants (Kuila et al., 2012). In present study, graphene precursors were chemically functionalised to enhance their adsorptive properties. The effectiveness of the functionalised graphene as adsorbent for the removal of SA from aqueous solutions was evaluated in batch mode. Adsorption equilibrium data were analysed by several theoretical isotherm models.

2. Methodology

Graphene flakes of thicknesses 12 nm (C12) and 60 nm (C60) were obtained from Graphene Lab. Inc., USA in powder form. The materials were characterised by scanning electron microscope (SEM, Quanta 400F), accelerated surface area and porosimeter (ASAP, Micromeritics 2010) and Fourier transform infrared (FTIR) spectrophotometer (Perkin-Elmer Spectrum RXI). The graphenes were treated with chemical reagents *viz.* H_2SO_4 , HNO_3 , NaOH and KOH, in a reflux reactor consisting of a round bottom flask connected to a glass condenser (0.3 m) and mounted on a heating mantle. 0.1 g of graphene was reacted with 100 mL of 1 mol/L reagent at 353 K for 4 h. Thereafter, the carbon product was rinsed with distilled water until the pH of solution was approximately 7. The solids were separated from solution by filtration through filter paper (Sartorius, Grade 391) and dried in oven (Memmert) for 24 h. The final treated graphene was stored in desiccator at room temperature for use in subsequent tests.

Batch experiments were carried out to determine adsorption of SA onto prepared nanosorbents. A series of 20 mL SA solutions with concentration ranging from 20 to 50 mg/L were prepared in 50 mL conical flasks. 10 mg of nanosorbent was added into each solution. The solutions were agitated in waterbath shaker (Protech) at 100 rpm and 298 K for 12 h. Thereafter, the solution was filtered through the filter paper and SA concentration of the filtrate was determined by UV-Vis spectrophotometer (Perkin-Elmer Lambda 25) at maximum absorbance of 295 nm. The percentage removal (R , %), and adsorption capacity (q_e , mg/g), were determined by Eq(1) and Eq(2):

$$R = \frac{C_0 - C_e}{C_0} \times 100\% \quad (1)$$

$$q_e = \frac{(C_0 - C_e)V}{W} \quad (2)$$

where C_0 and C_e (mg/L) are the initial and final concentrations, respectively, V (L) is the solution volume and W (g) is the adsorbent mass.

Adsorption isotherm models *viz.* Langmuir, Temkin and Dubinin-Radushkevich (D-R), were used to describe the equilibrium distribution of SA in aqueous medium and adsorbent at a fixed temperature. Langmuir model describes the monolayer adsorption of adsorbate on homogenous sites without any interactions between adsorbed molecules. This model is represented by Eq(3) (Langmuir, 1918):

$$q_e = \frac{q_m K_L C_e}{1 + K_L C_e} \quad (3)$$

where q_m (mg/g) is the maximum adsorption capacity and K_L (L/mg) is the Langmuir binding energy. Temkin model considers a linear reduction in the adsorption energy content with an increase in the degree of completion of the sorption sites (Temkin and Pyzhev, 1940). The model is expressed by Eq(4):

$$q_e = \frac{RT}{B} \log AC_e \quad (4)$$

where A (L/mg) and B (J/mol) are Temkin constants related to the maximum binding energy and variation of adsorption heat, respectively, R (8.314 J/mol K) is the universal gas constant and T (K) is the absolute temperature. D-R model assumes heterogeneous surface sorption process and is represented by Eq(5) (Dubinin and Radushkevich, 1947):

$$q_e = X_m \exp(-\beta \varepsilon^2) \quad (5)$$

where X_m (mg/g) is the adsorption capacity, β (g^2/J^2) is the activity coefficient related to adsorption energy, ε ($=RT/M \log(1+1/C_e)$, J/g) is the Polanyi potential and M (g/mol) is the adsorbate molar weight. Freundlich

model assumes an exponential reduction of adsorption energy with the increase in surface coverage (Freundlich, 1906). It is expressed by Eq(6):

$$q_e = K_F C_e \exp(1/n) \quad (6)$$

where K_F ((mg/g)(L/mg)^{1/n}) is the Freundlich constant and n is the Freundlich exponent.

The model parameters were determined by non-linear regression using Microsoft Excel Solver. The fit of the model to the experimental data was evaluated by error functions such as Marquardt's percent standard deviation (MPSD), chi-square (χ^2), average relative error (ARE) and sum of absolute error (SAE) which are given by Eq(7)-Eq(10) (Montgomery, 2011):

$$MPSD = 100 \sqrt{\frac{1}{n_s - p} \sum_{i=1}^N \left(\frac{q_{e,exp} - q_{e,cal}}{q_{e,exp}} \right)^2} \quad (7)$$

$$\chi^2 = \sum_{i=1}^N \frac{(q_{e,cal} - q_{e,exp})^2}{q_{e,exp}} \quad (8)$$

$$ARE = \frac{100}{n_s} \sum_{i=1}^N \left| \frac{q_{e,exp} - q_{e,cal}}{q_{e,exp}} \right| \quad (9)$$

$$SAE = \sum_{i=1}^N |q_{e,cal} - q_{e,exp}| \quad (10)$$

where $q_{e,cal}$ (mg/g) and $q_{e,exp}$ (mg/g) are the calculated and experimental equilibrium adsorption capacities, respectively, n_s is the number of data and p is the number of isotherm parameters. As the non-linear regression produces different sets of parameters based on different error functions, optimisation procedure was performed using the sum of normalised errors (SNE) described by Ho et al. (2002). Accordingly, the parameter set exhibiting the smallest SNE is to be selected as the optimum model parameters.

3. Results and discussion

Figure 1 shows the SEM images of C12 and C60 at magnification of 5,000x. The graphenes exhibit layered structure with smooth surface, and irregular and wrinkle edges. EDX analysis indicated that C12 consists of pure carbon while C60 consists of 90.31 % carbon, 7.94 % oxygen and 1.75 % sulphur. N₂ adsorption analysis at 77 K revealed that the Brunauer–Emmett–Teller specific surface area of C12 was 68.74 m²/g and that of C60 was 9.76 m²/g.

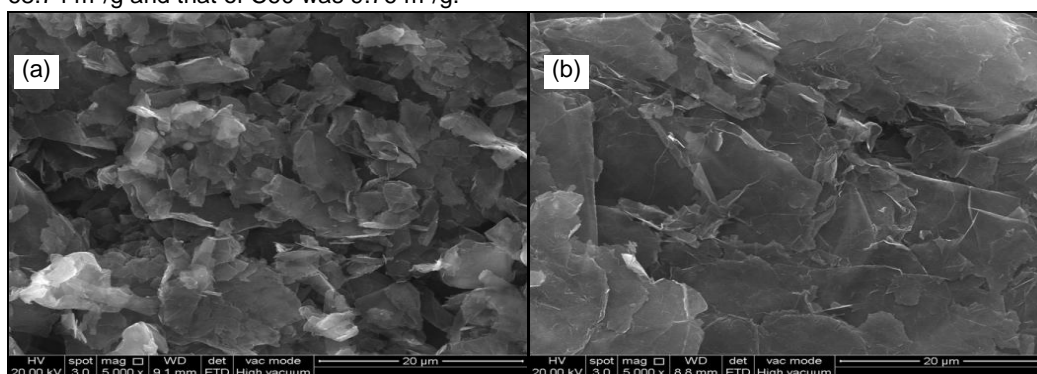


Figure 1: SEM images of C12 (a) and C60 (b) at magnification of 5,000x

Figure 2 depicts the percentage removal of SA by C12 and C60 functionalised with different reagents. As can be seen, C12-H₂SO₄ exhibited the highest percentage removal of SA. This finding suggests that H₂SO₄ is the most appropriate reagent for the functionalisation of graphene in the current study. The percentage removal decreases in the following order with respect to reagents used for functionalising C12 and C60: C12-H₂SO₄ > C60-H₂SO₄ > C60-KOH > C12-NaOH > C60-HNO₃ > C12-KOH > C60-KOH >

$C_{12}\text{-HNO}_3 > C_{12} > C_{60}$. The natural pH of SA solution was 3.8. At this low pH condition, the adsorbent surface was protonated by H^+ ions resulting in a positively charged surface. Therefore, SA removal by the functionalised graphene might be due to electrostatic attraction between the adsorbent and SA anions. The results indicated that $C_{12}\text{-H}_2\text{SO}_4$ has potential application in treating aqueous effluent contaminated by SA and hence, is worthy of further investigation.

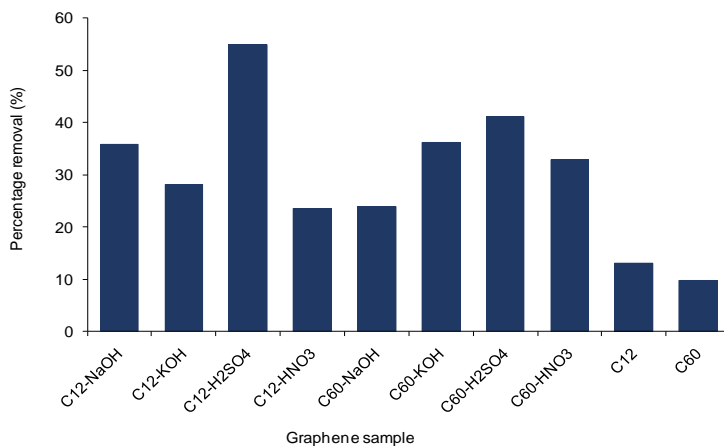


Figure 2: Percentage removal of SA by different functionalised graphenes

The FTIR spectra of C12 and C12-H₂SO₄ are presented in Figure 3. There is no distinct peak present in the spectrum of C12. The spectrum of C12-H₂SO₄ exhibits a broad peak at $3,402\text{ cm}^{-1}$ indicating the presence of hydroxyl group and peaks at $2,371$, $1,637$, $1,284$ and $1,176\text{ cm}^{-1}$ caused by stretching vibrations in alkyne, amine, carboxylic acid and carbonyl groups, respectively. Further peaks at $1,069$ and $1,007\text{ cm}^{-1}$ were due to stretching vibrations in alcohol and alkyl halide groups, respectively.

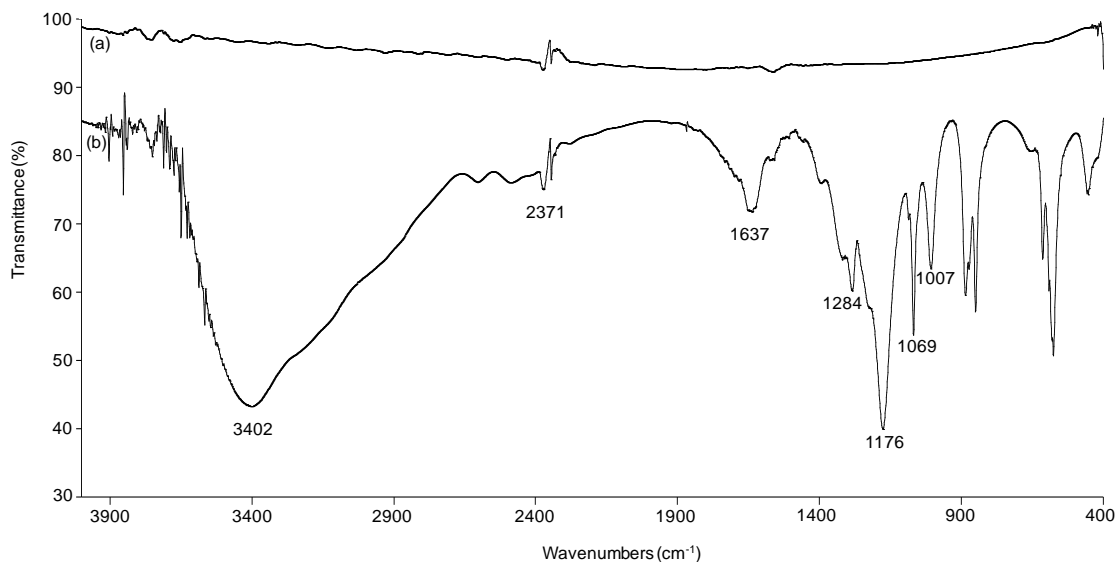


Figure 3: FTIR spectra of C12 (a) and C12-H₂SO₄ (b)

The effect of initial concentration on the removal of SA by C12-H₂SO₄ was evaluated between 20-50 mg/L. Figure 4 shows that the removal percentage increases with an increase in the initial concentration until equilibrium was reached. This indicates that an increase in initial concentration resulted in a stronger driving force to overcome the mass transfer resistances of SA between liquid and solid phases.

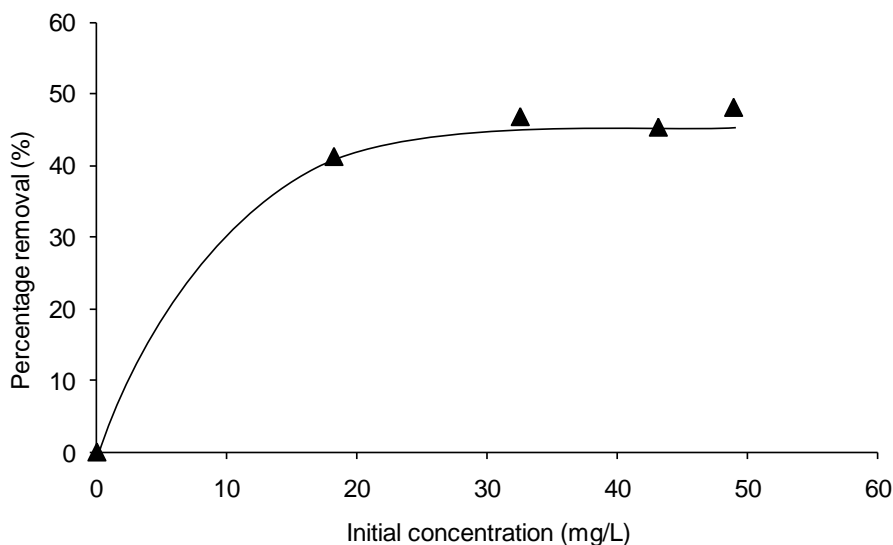


Figure 4: Percentage removal of SA by C12-H₂SO₄

The equilibrium experimental data were fitted to Langmuir, Temkin, D-R and Freundlich models by non-linear regression. The deviation of experimental data from model predictions was minimised by error functions such as *MPSD*, χ^2 , *ARE* and *SAE*. The isotherm plots of both the experimental and predicted values are presented in Figure 5. The calculated model parameters based on different error functions are summarised in Table 1.

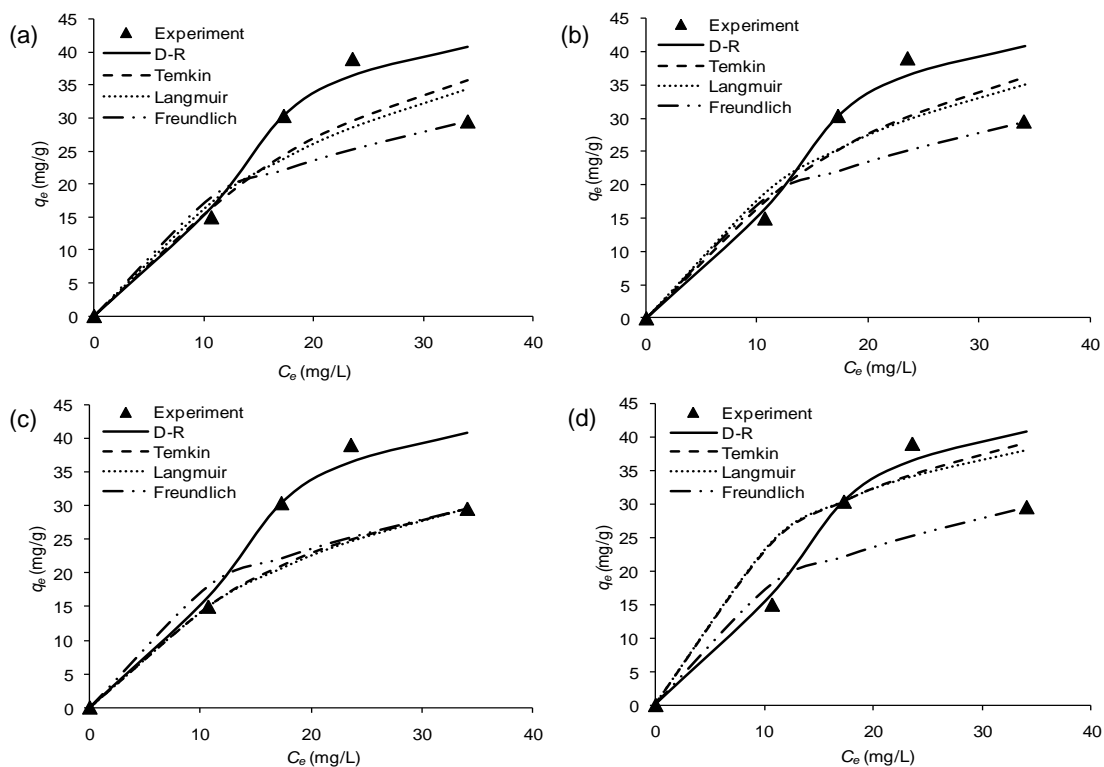


Figure 5: Comparison of experimental and predicted isotherms of SA adsorption onto C12-H₂SO₄ based on *MPSD* (a), χ^2 (b), *ARE* (c) and *SAE* (d)

On the basis of the lowest SNE value for χ^2 (0.7551), D-R model provided the best fit for the experimental data. The suitability of D-R model indicates that SA anions are attached onto heterogeneous surface of C12-H₂SO₄. The X_m and B values were found to be 38.51 mg/g and 0.3328 g²/J².

Table 1: SNE analysis for Langmuir, Temkin, D-R and Freundlich models.

Model	Model parameters	Error Function			
		MPSD	χ^2	ARE	SAE
Langmuir	$q_m(\text{mg/g})$	63.66	57.75	53.17	51.26
	$K_L(\text{L/mg})$	0.0346	0.0451	0.0366	0.0838
	SNE	3.9805	0.9416	2.3488	3.3753
Temkin	$B(\text{J/mol})$	148.43	154.32	197.60	190.70
	$A(\text{L/mg})$	0.2477	0.2782	0.3084	0.5975
	SNE	3.9676	0.9393	2.3345	3.4335
D-R	$X_m(\text{mg/g})$	38.07	38.51	48.19	45.34
	$B(\text{g}^2/\text{J}^2)$	0.3447	0.3328	0.4557	0.3956
	SNE	3.9854	0.7551	2.1381	3.2306
Freundlich	$K_F((\text{mg/g})(\text{L/mg})^{1/n})$	4.05	5.32	3.08	6.55
	n	1.640	1.864	1.499	2.344
	SNE	3.9782	1.0254	2.4789	3.7883

4. Conclusion

Functionalisation of graphene with chemical reagents, such as H_2SO_4 , HNO_3 , NaOH and KOH , was successfully carried out using reflux method. The results showed that graphene functionalised with H_2SO_4 was the most effective nanosorbent for adsorption of SA in aqueous media. Non-linear regression analysis on equilibrium data revealed that SA adsorption was best described by D-R model which exhibited the lowest SNE (0.7551).

Acknowledgements

This work was supported by Ministry of Science, Technology and Innovation (MOSTI) Malaysia under the Grant No. 06-02-12-SF0224.

References

- Alvarez S., Sotelo J.L., Ovejero G., Rodriguez A., Garcia J., 2013, Low-cost adsorbent for emerging contaminant removal in fixed-bed columns, *Chemical Engineering Transactions*, 32, 61-66.
- Dubin M.M., Radushkevich L.V., 1947, The equation of the characteristic curve of the activated charcoal, *Proc. Acad. Sci. USSR*, 55, 331-333.
- Essandoh M., Kunwar B., Pittman Jr.C.U., Mohan D., Misra T., 2015, Sorptive removal of salicylic acid and ibuprofen from aqueous solutions using pine wood fast pyrolysis biochar, *Chem. Eng. J.*, 265, 219-227.
- Freundlich H.M.F., 1906, Over the adsorption in solution, *J. Phys. Chem.* 57, 385-470.
- Ho Y.S., Porter J.F., McKay G., 2002, Equilibrium isotherm studies for the sorption of divalent metal ions onto peat: copper, nickel and lead single component systems, *Water Air Soil Poll.*, 141, 1-33.
- Jiang J.Q., Zhou Z., Sharma V.K., 2013, Occurrence, transportation, monitoring and treatment of emerging micro-pollutants in waste water - A review from global views, *Microchem. J.*, 110, 292-300.
- Kuila T., Bose S., Mishra A.K., Khanra P., Kim N.H., Lee J.H., 2012, Chemical functionalisation of graphene and its applications, *Prog. Mater. Sci.*, 57, 1061-1105.
- Langmuir I., 1918, The adsorption of gases on plane surfaces of glass, mica and platinum, *J. Am. Chem. Soc.*, 40, 1361-1403.
- Martucci A., Pasti L., Marchetti N., Cavazzini A., Dondi F., Alberti A., 2012, Adsorption of pharmaceuticals from aqueous solutions on synthetic zeolites, *Micropor. Mesopor. Mat.*, 148, 174-183.
- Montgomery D.C., 2011, *Design and Analysis of Experiments*, John Wiley & Sons, New York, USA.
- Otero M., Grande C.A., Rodrigues A.E., 2004, Adsorption of salicylic acid onto polymeric adsorbents and activated charcoal, *React. Funct. Polym.*, 60, 203-213.
- Temkin M.I., Pyzhev V.M., 1940, Kinetics of ammonia synthesis on promoted iron catalyst, *Acta Physiochim. USSR.*, 12, 327-356.
- Turku I., Sainio T., Paatero E., 2009, Adsorption of 17β -estradiol onto two polymeric adsorbents and activated carbon, *Chemical Engineering Transactions*, 17, 1555-1560.